Copy

RM A58E21a

NACA RM A58E21a

NACA

RESEARCH MEMORANDUM

FORCES AND PITCHING MOMENTS ON AN ASPECT-RATIO-3.1 WING-BODY COMBINATION AT MACH NUMBERS FROM 2.5 TO 3.5 AND SUBLIMATION STUDIES OF THE EFFECT OF SINGLE-ELEMENT ROUGHNESS ON THE BOUNDARY-LAYER FLOW

By Edward J. Hopkins, Stephen J. Keating, Jr.,
and Richard R. Muhl

Ames Aeronautical Laboratory
Moffett Field, Calif.

NATIONAL ADVISORY COMMITTEE
FOR AERONAUTICS

WASHINGTON

August 26, 1958

Declassified January 12, 1961

NATIONAL ADVISORY COMMITTEE FOR AERONAUTICS

RESEARCH MEMORANDUM

FORCES AND PITCHING MOMENTS ON AN ASPECT-RATIO-3.1 WING-BODY COMBINATION AT MACH NUMBERS FROM 2.5 TO 3.5 AND SUBLIMATION STUDIES OF THE EFFECT OF SINGLE-ELEMENT ROUGHNESS ON THE BOUNDARY-LAYER FLOW*

By Edward J. Hopkins, Stephen J. Keating, Jr.,
and Richard R. Muhl

SUMMARY

Lift, drag, and pitching-moment characteristics for a wing-body combination are presented throughout a Mach number range from 2.49 to 3.53. The wing had an aspect ratio of 3.1, a sweepback of the leading edge of 19.1°, a taper ratio of 0.39, and a biconvex profile with a thickness of 3 percent of the chord. Linear theory with account taken of the mutual interference between the wing and the body gave a good estimate of the variation of the lift and pitching-moment curve slopes with Mach number.

Photographs taken during a visual-flow study by the sublimation technique are presented for the model equipped with various sizes of single-element roughness. At a Mach number of 3.53 and Reynolds number of 1.3×10^6, none of the roughness elements tested were effective in producing transition. The tests indicated that a single-element roughness large enough to fix transition at the element would create a drag increment over four times the additional skin-friction drag associated with the increased extent of turbulent boundary layer. Each roughness element produced what appeared to be small regularly spaced streamwise vortices in the boundary layer.

INTRODUCTION

A program is currently in progress in which the same wing-body combination is being tested throughout a Mach number range from subsonic to high supersonic speeds in various wind tunnels at Ames Aeronautical Laboratory. These investigations have been conducted primarily to provide experimental force and moment data over a large Mach number range and to provide information for comparisons of data obtained at the same

*Title, Unclassified.

Mach and Reynolds numbers from the same model in different wind tunnels. Experimental results from some of the investigations reported upon thus far are contained in references 1 to 5. Force and moment data are presented herein throughout a Mach number range from 2.49 to 3.53.

In several supersonic wind-tunnel investigations it has been the practice to produce boundary-layer transition on the model near the wing leading edge in an attempt to obtain flow conditions within the boundary layer believed to be more representative of flight conditions. At Mach numbers below about 2.5 considerable information exists on the minimum size of roughness element required to produce transition on bodies of revolution and on wings (e.g., refs. 6 and 7), but only a limited amount of information is available at the higher Mach numbers. To provide some information on the roughness requirement at a Mach number of 3.53, results from a visual-flow study are presented for the model equipped with various sizes of single-element roughness.

NOTATION

C_L lift coefficient, $\frac{\text{lift}}{qS}$

C_{L_α} lift curve slope measured at $\alpha = 0^\circ$

C_D drag coefficient, $\frac{\text{drag}}{qS}$

C_m pitching-moment coefficient, $\frac{\text{pitching moment}}{qS\bar{c}}$

$\left(\frac{dC_m}{dC_L}\right)_{C_L=0}$ pitching-moment curve slope measured at $C_L = 0$

b wing span

$\bar{c}$ mean aerodynamic chord, $\dfrac{\int_0^{b/2} c^2 dy}{\int_0^{b/2} c\, dy}$

c local chord

$\frac{L}{D}$	lift-to-drag ratio
M	Mach number
q	free-stream dynamic pressure
R	Reynolds number based on $\overline{c}$
S	wing area
y	lateral distance from the body axis
α	angle of attack

APPARATUS

Wind Tunnel

Tests were conducted in the 8- by 7-foot supersonic test section of the Ames Unitary Plan Wind Tunnel. The Mach number in this test section can be set at any value from 2.5 to 3.5 by the movement of flexible nozzle walls while the wind tunnel is in operation. The pressure is automatically maintained at any selected value between 5 and 55 inches of mercury absolute. A more detailed description of this wind tunnel is given in reference 8.

Model

The model consisted of a wing-body combination and was mounted on a six-component strain-gage balance which was attached to a sting support. A photograph of the model mounted in the wind tunnel is shown in figure 1. The wing had an aspect ratio of 3.1, a taper ratio of 0.39, and a leading-edge sweepback of 19.1°. The wing profile was biconvex with a maximum thickness of 3 percent of the chord. The equation given in figure 2, which defines the body of revolution, was derived by W. R. Sears and W. Haack and satisfies the theoretical criteria for minimum wave drag at supersonic speeds for a closed body with a given length and volume. Complete dimensional data for the model are given in figure 2.

TEST METHODS AND TECHNIQUES

Force-Test Variables

Measurements of the forces and pitching moments at Mach numbers of 2.49, 2.78, 3.06, 3.29, and 3.53 were made by means of a six-component electrical strain-gage balance. For each Mach number the tests were conducted at Reynolds numbers of 1.3 and 2.5 million. In order to increase the positive angle-of-attack range the model was supported on a sting which had a bend angle of 13°. For each test condition the model was pitched through an angle-of-attack range of -1.0° to 27.7°.

Reduction of Data

Corrections.- The axial forces used to compute the drag coefficients were adjusted to the condition of having the free-stream static pressure on the base of the model.

An incremental Mach number was added to the nominal Mach number setting to account for the small longitudinal gradient of Mach number in the wind tunnel. The Mach number variation along the tunnel center line over the model length was less than 0.05. The Mach numbers presented in the figures are for the longitudinal station which corresponds to the intersection of the wire leading edge and the body surface.

Accuracy.- The accuracies listed below are based on the least counts of the read-out equipment and the repeatability of the measuring systems.

C_L	± 0.015
C_m	± 0.004
C_D	± 0.0013
α	$\pm 0.05^{\circ}$
M	± 0.01
R	$\pm 0.05 \times 10^6$

Roughness Sizes

In general, as the Mach number increases and/or the Reynolds number per unit length decreases, the element size required for transition

increases, as indicated by references 6 for bodies of revolution and 7 for wings. Although not strictly applicable, these references were used as a guide in the selection of element sizes for the present investigation. Accordingly, 0.032-, 0.051-, 0.063-, and 0.093-inch-diameter wires were attached to the wing surfaces at the chordwise positions shown in figure 3. The 0.063-inch roughness element corresponds approximately to the size required to fix transition at the element at a Mach number of 3.53 and a Reynolds number of 1.3 million, according to an extrapolation of the data of reference 7. This choice of Mach and Reynolds numbers represented the most severe test condition for fixing transition of those covered in the force tests. Only the 0.063-inch roughness element was investigated on the body at the location shown in figure 3.

Visual-Flow Technique

The sublimation technique of reference 9 was chosen as the simplest and the best suited method of flow visualization for the test conditions encountered in the present investigation. In selection of the sublimable material, the time required to bring the wind tunnel up to operating conditions is an important factor, about 40 minutes for the present tests; the material selected was azobenzene ($C_6H_5N{:}NC_6H_5$). To preserve the lacquer finish on the model petroleum ether was chosen as the carrying agent.

The rate of sublimation is affected by the local temperature of the sublimable solid and by the shear near the material. Therefore, the sublimer evaporates more rapidly for a turbulent boundary layer than for a laminar boundary layer except near the wing leading edge where the shear is high.

RESULTS AND DISCUSSION

Aerodynamic Characteristics

The lift, drag, pitching-moment, and lift-drag-ratio results at two Reynolds numbers are presented throughout the Mach number range of 2.49 to 3.53 in figure 4. Summary plots of important aerodynamic characteristics as a function of Mach number are presented in figure 5. Since a change in Reynolds number from 1.3 to 2.5 million had a negligible effect on the result, a single curve is presented for both Reynolds numbers on the summary plots. To indicate the general agreement between the present results and those from another facility, data from reference 1 have also been included in figure 5. In addition, the aerodynamic center and the lift curve slope, calculated by the linear theory of references 10 and 11, are also shown in figure 5.

Linear theory gave a good estimate of the variation of lift and pitching-moment curve slopes with Mach number. However, small differences between the experimental and theoretical values of these slopes can be noted.

At a constant lift coefficient, the drag coefficient increased about 35 percent with an increase in Mach number from 2.49 to 3.53. The maximum lift-drag ratio decreased from about 6.0 to 4.8 over this same Mach number range. Inspection of the drag results indicates that the induced drag due to lift was approximately equal to the lift times the angle of attack, the expected result for a wing having a supersonic leading edge.

Visual-flow studies, described hereinafter, indicated that laminar flow existed over the entire wing at $\alpha = 0^\circ$ and a Mach number of 3.53, the only Mach number at which these studies were made. No force measurements are presented for the model with roughness elements attached to the wing surfaces, since preliminary force tests indicated that the element size required to fix transition at the element would create an excessively large wave drag. Although the largest roughness element investigated, the 0.093-inch element, did not produce turbulent flow over the entire wing, this element created a drag increment which was about four times as large as the drag increment estimated for the difference between having completely turbulent and completely laminar flow on the wing.

Visual-Flow Studies

Sublimation photographs taken with the model at $\alpha = 0^\circ$ at certain time intervals after the wind tunnel was brought up to operating speed and pressure are presented in figure 6. The time intervals are shown on each photograph.

Figures 6(a) and 6(b) indicate that laminar flow existed over nearly the entire "smooth" wing at either Reynolds number except near the wing-body juncture and the wing tip. At the lower Reynolds number of 1.3 million each roughness element appeared to be ineffective in producing a turbulent boundary layer outside of the shock wave which emanates from the body nose and to have questionable effectiveness within this bow wave. At the higher Reynolds number of 2.5 million, the three roughness elements produced transition at the element within the bow wave and at some distance behind the element outside the wave as evidenced by figures 6(b) and 6(d). Although the photographs at a Reynolds number of 2.5 million were taken 24 minutes later than those at a Reynolds number of 1.3 million, because of the time required to increase the wind-tunnel pressure, complete time histories of the sublimation progression indicate that the photographs at the higher Reynolds number are indicative of the flow conditions existing on the wing at this Reynolds number. Differences in the effectiveness of the roughness in producing transition outside of

and within the bow wave can be attributed to the existence of higher local Reynolds numbers within this wave because of the density changes and the excitation of flow fluctuations associated with the flow through the body bow wave. The 0.063-inch roughness element on the body nose fixed transition approximately halfway between the element and the wing-body juncture at a Reynolds number of 1.3 million, but at the element at a Reynolds number of 2.5 million, as indicated by figures 6(c) and 6(d).

The striations which are visible in the photographs suggest that vortices having their axes in the stream direction are created by the flow over the wire. Measurements made on the photographs under a magnifying glass indicated that the vortex spacing became smaller with a decrease in wire height and/or with the increase in Reynolds number found inside the bow wave. Similar striations have been mentioned in previous investigations on swept wings (refs. 7 and 12), on concave curved surfaces (refs. 13, 14, and 15), and on rotating discs (ref. 12). In reference 16 it was demonstrated that vortices can be produced by a wire attached to a flat plate but that the effective curvature of the stream lines induced by this element forward of the element is insufficient to produce the vortices according to Görtler's theory (refs. 14 and 15). The vortices in the present investigation may have been produced by either the effect of a concave curvature of the boundary-layer flow immediately behind the wire or by the three-dimensional flow induced by the sweep of the wire by a mechanism similar to that mentioned in reference 12.

CONCLUDING REMARKS

Linear theory with the mutual interference between the wing and the body taken into account gave a good estimate of the variation of the lift and pitching-moment curve slopes with Mach number.

Limited drag measurements made at a Mach number of 3.53 and a Reynolds number of 1.3 million indicated that the size of the single-element roughness required to fix transition at the element was so large as to create a drag increment about four times the additional skin-friction drag associated with a turbulent boundary layer. Flow over the wire produced what appeared to be vortical flow in the form of small regularly spaced vortices with their axes alined with the stream direction. Further investigations will be required to establish whether the effective curvature of the boundary-layer flow behind a wire can produce vortices or whether a swept wire on a surface can produce vortices similar to those found on swept wings.

Ames Aeronautical Laboratory
National Advisory Committee for Aeronautics
Moffett Field, Calif., May 21, 1958

REFERENCES

1. Hall, Charles F.: Lift, Drag, and Pitching Moment of Low-Aspect-Ratio Wings at Subsonic and Supersonic Speeds. NACA RM A53A30, 1953.

2. Stivers, Louis S., Jr., and Lippmann, Garth W.: Effects of Vertical Locations of Wing and Horizontal Tail on the Aerodynamic Characteristics in Pitch at Mach Numbers From 0.60 to 1.40 of an Airplane Configuration With an Unswept Wing. NACA RM A58I10, 1957.

3. Knechtel, Earl D., and Summers, James L.: Effects of Sweep and Taper Ratio on the Longitudinal Characteristics of an Aspect Ratio 3 Wing-Body Combination at Mach Numbers From 0.6 to 1.4. NACA RM A55A03, 1955.

4. Smith, Donald W., Shibata, Harry H., and Selan, Ralph: Lift, Drag, and Pitching Moment of Low-Aspect-Ratio Wings at Subsonic and Supersonic Speeds - An Investigation at Large Reynolds Numbers of the Low-Speed Characteristics of Several Wing-Body Combinations. NACA RM A51K28, 1952.

5. Hunton, Lynn W.: Effects of Fixing Transition on the Transonic Aerodynamic Characteristics of a Wing-Body Configuration at Reynolds Numbers From 2.4 to 12 Million. NACA TN 4279, 1958.

6. Luther, Marvin: Fixing Boundary-Layer Transition on Supersonic-Wind-Tunnel Models. J.P.L. Progress Rep. No. 20-287, C.I.T., Pasadena, Calif., Feb. 1, 1956. (Supersedes Ibid. Progress Rep. 20-256, Aug. 12, 1955)

7. Winter, K. G., Scott-Wilson, J. B. (N.A.E.), and Davies, F. V.: Methods of Determination and of Fixing Boundary Layer Transition on Wind Tunnel Models at Supersonic Speeds. British A.R.C. C.P. 212 (17,416) 1955. (Supersedes R.A.E. TN No. Aero. 2341, Sept. 1954)

8. Huntsberger, Ralph F., and Parsons, John F.: The Design of Large High-Speed Wind Tunnels. NACA paper presented at Fourth General Assembly of the AGARD Wind-Tunnel Panel, Scheveningen, The Netherlands, AG 15/p6, May 3-7, 1954.

9. Main-Smith, J. D.: Chemical Solids as Diffusible Coating Films for Visual Indication of Boundary-Layer Transition in Air and Water. British A.R.C. R.&M. 2755, 1954. (Also issued as R.A.E. Chem. 466, 1950)

10. Pitts, William C., Nielsen, Jack N., and Kaattari, George E.: Lift and Center of Pressure of Wing-Body-Tail Combinations at Subsonic, Transonic, and Supersonic Speeds. NACA Rep. 1307, 1957.

11. Lagerstrom, P. A., Wall, D., and Graham, M. E.: Formulas in Three-Dimensional Wing Theory. Douglas Aircraft Co. Rep. SM 11901, 1946.

12. Gregory, N., Stuart, J. T., and Walker, W. S.: On the Stability of Three-Dimensional Boundary Layers With Application to the Flow Due to a Rotating Disc. Royal Soc. (Brit.), Philosophical Trans., ser. A, vol. 248, no. 943, July 14, 1955.

13. Gregory N., and Walker, W. S.: The Effect on Transition of Isolated Surface Excrescences in the Boundary Layer. British A.R.C., Fluid Motion Sub-Committee 13,436. (FM 1482, Perf. 698), Oct. 12, 1950.

14. Görtler, H.: On the Three-Dimensional Instability of Laminar Boundary Layers on Concave Walls. NACA TM 1375, 1954.

15. Görtler, H.: Instability of Laminar Boundary Layers on Concave Walls Against Certain Three-Dimensional Disturbances. Ministry of Aircraft Production, RTP Tr. 1588, Z.a.M.M., vol. 21, no. 4, Aug. 1941.

16. Hama, Francis R., Long, James D., and Hegarty, John C.: On Transition From Laminar to Turbulent Flow. Jour. Appl. Phys., vol. 28, no. 4, April 1957.

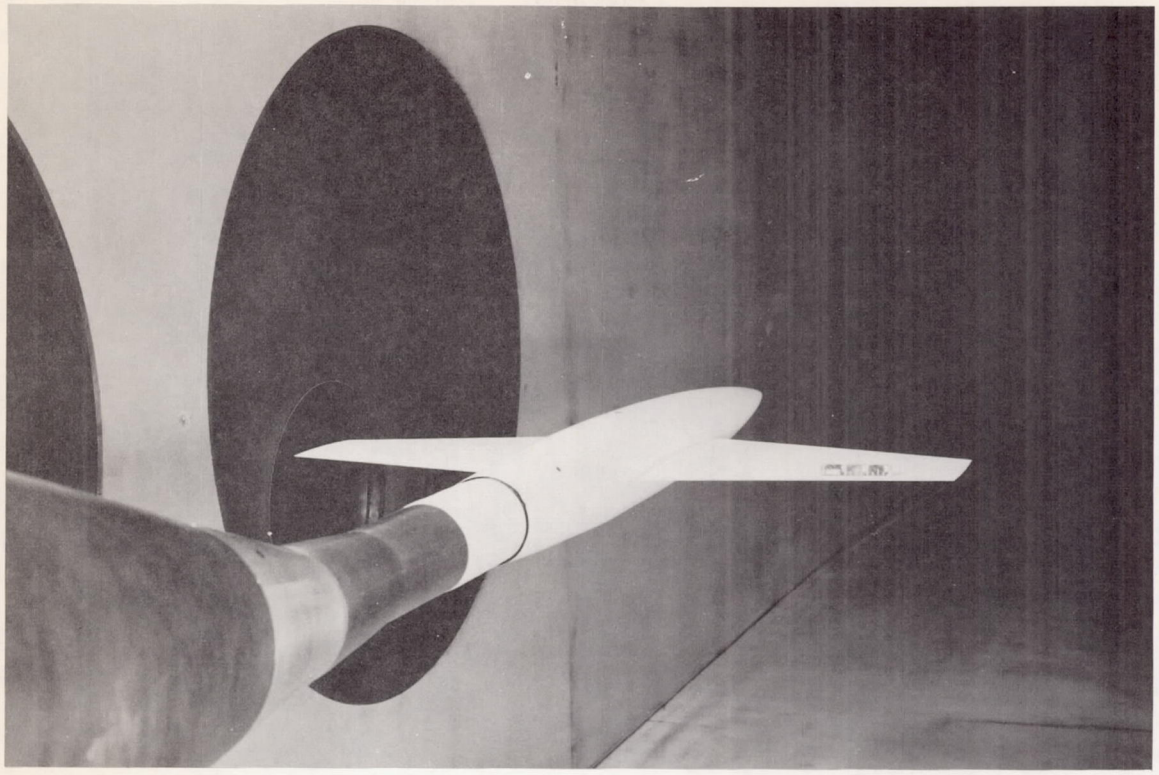

A-21896

Figure 1.- Model mounted in the 8- by 7-foot supersonic test section of the Ames Unitary Plan Wind Tunnel.

Equation of fuselage radii:

$$\frac{r}{r_o} = \left[1-\left(1-\frac{2x}{l}\right)^2\right]^{\frac{3}{4}}$$

All dimensions in inches.

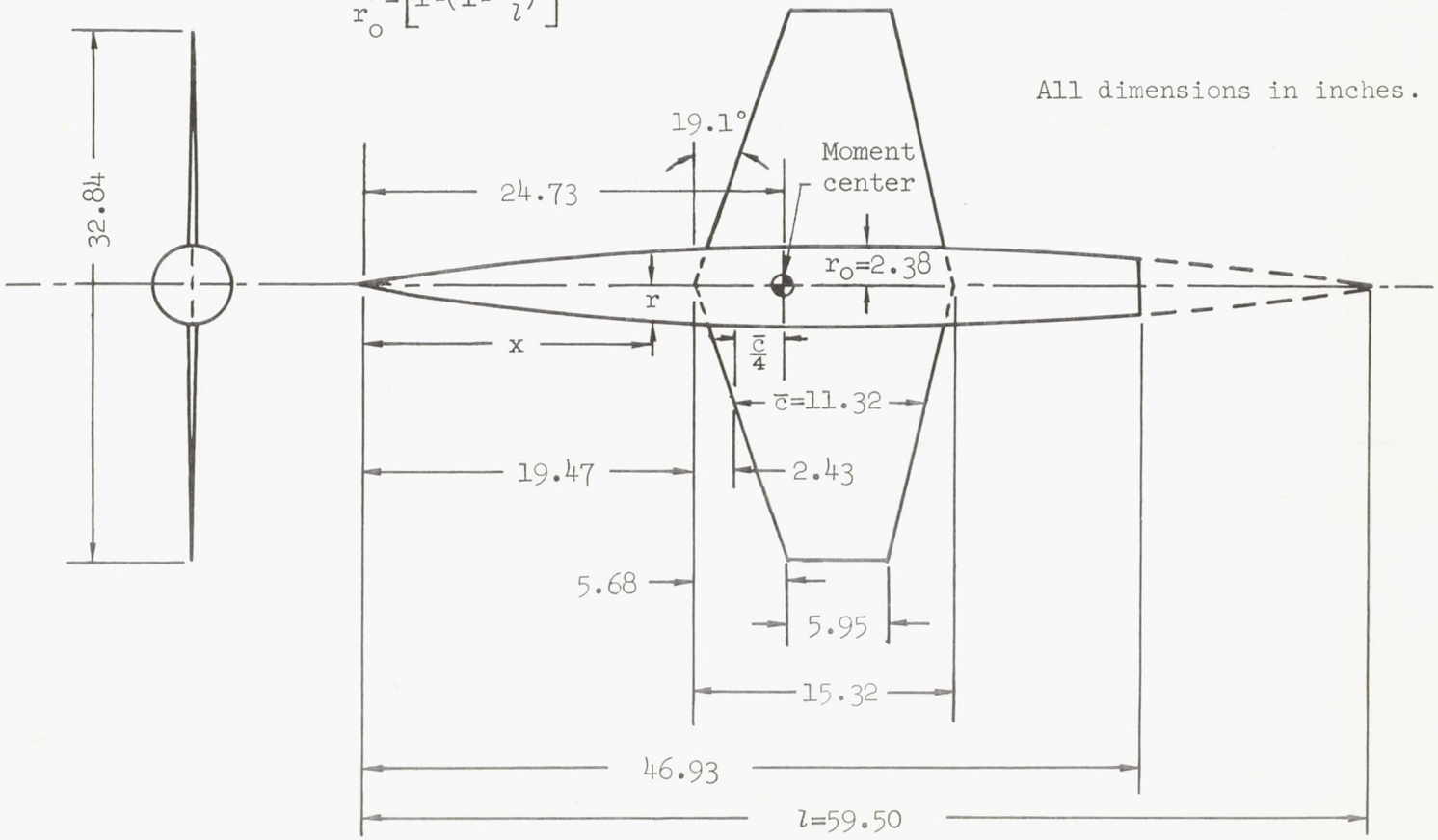

Figure 2.- Model dimensions.

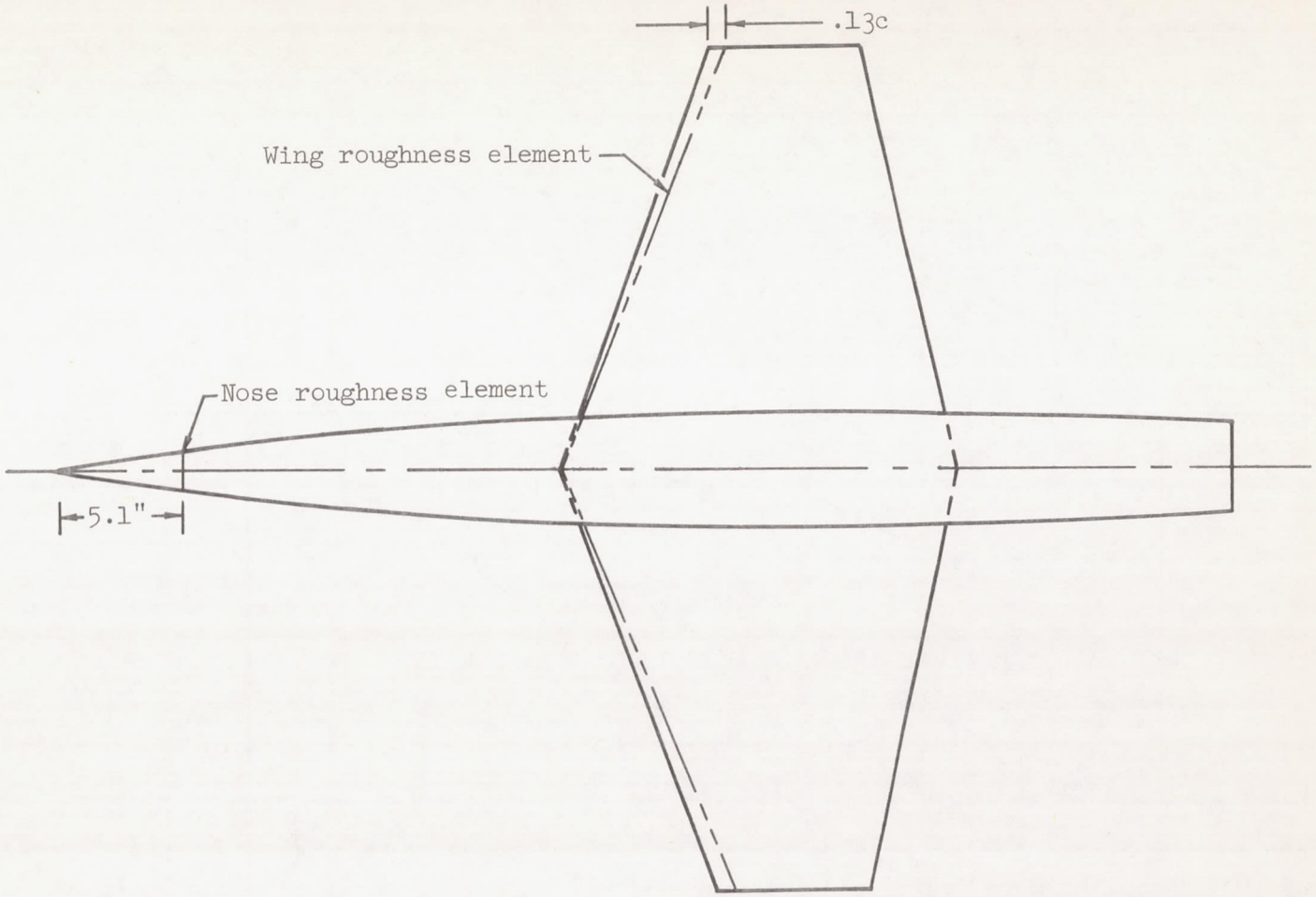

Figure 3.- Locations of the roughness elements.

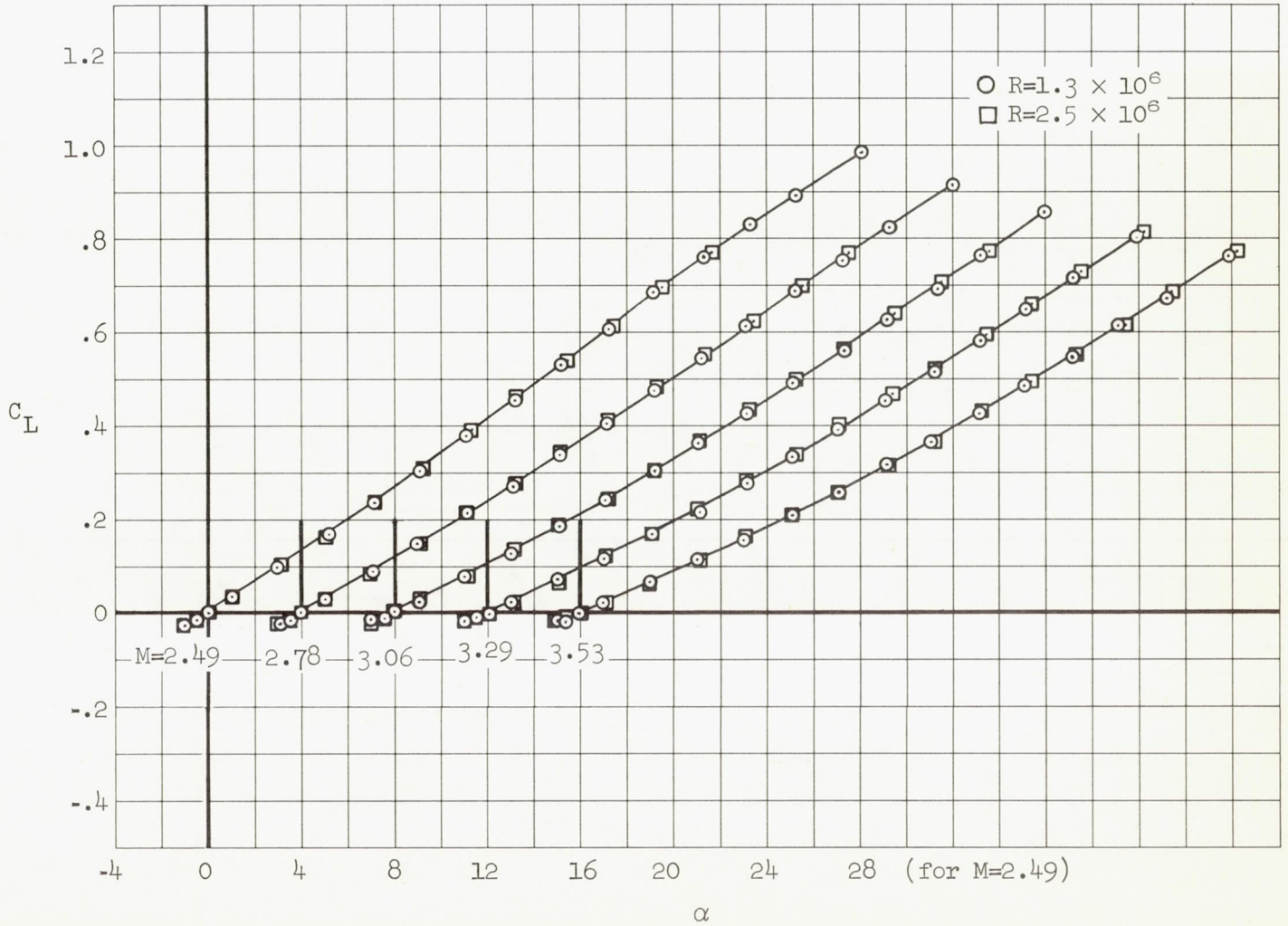

(a) C_L vs. α

Figure 4.- Lift, drag, pitching-moment, and lift-to-drag ratio characteristics; smooth wing.

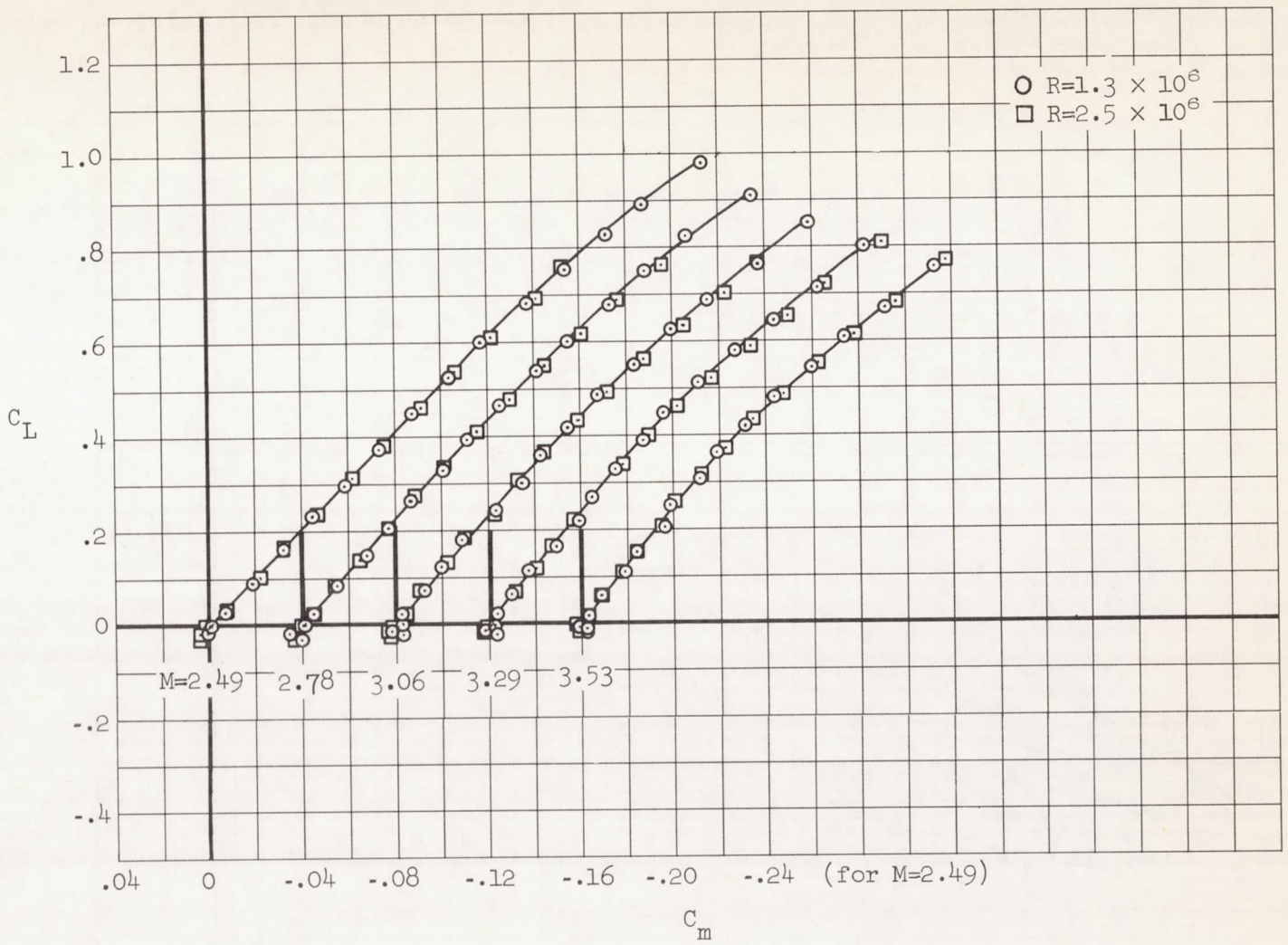

(b) C_L vs. C_m

Figure 4.- Continued.

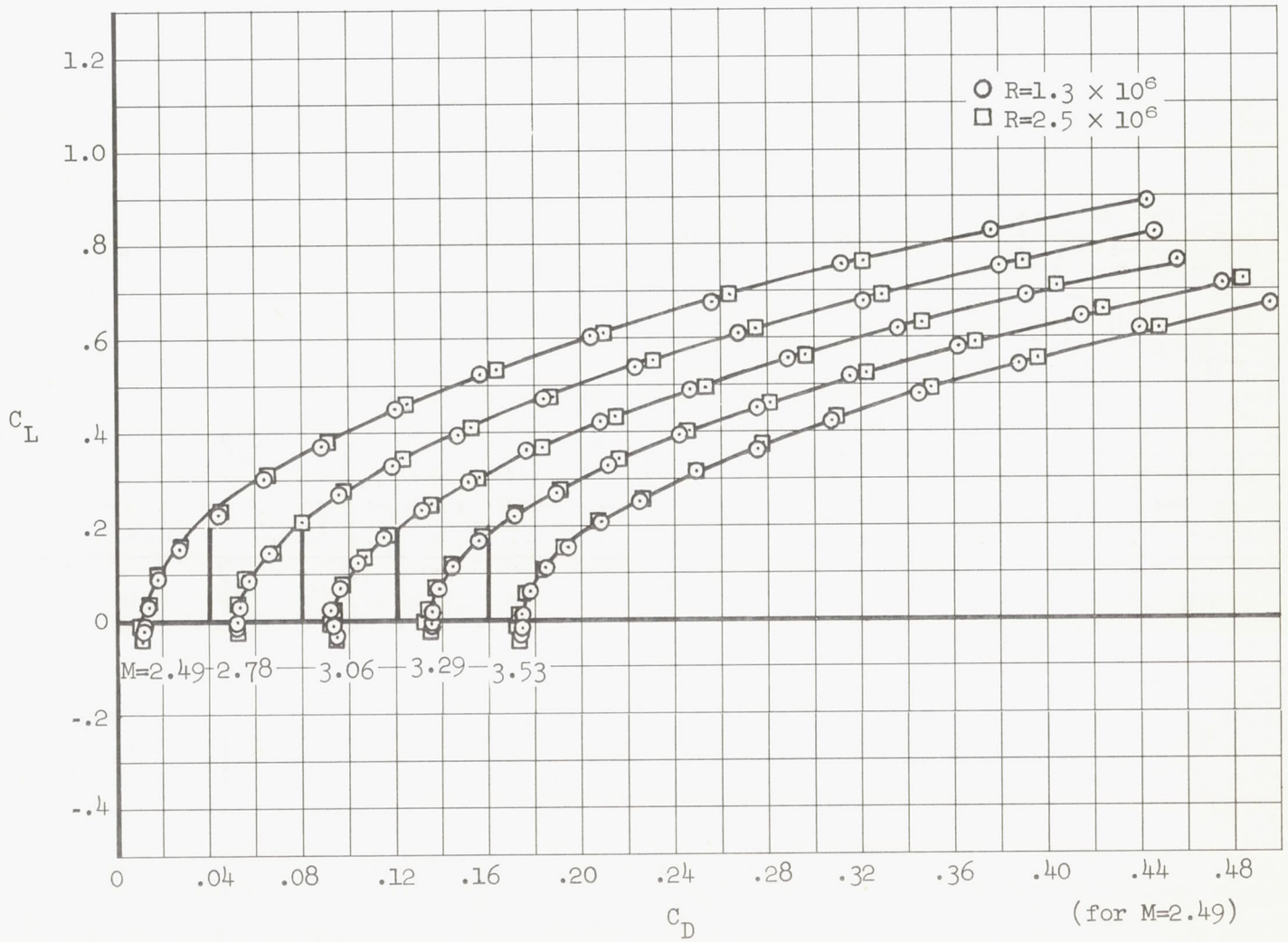

(c) C_L vs. C_D

Figure 4.- Continued.

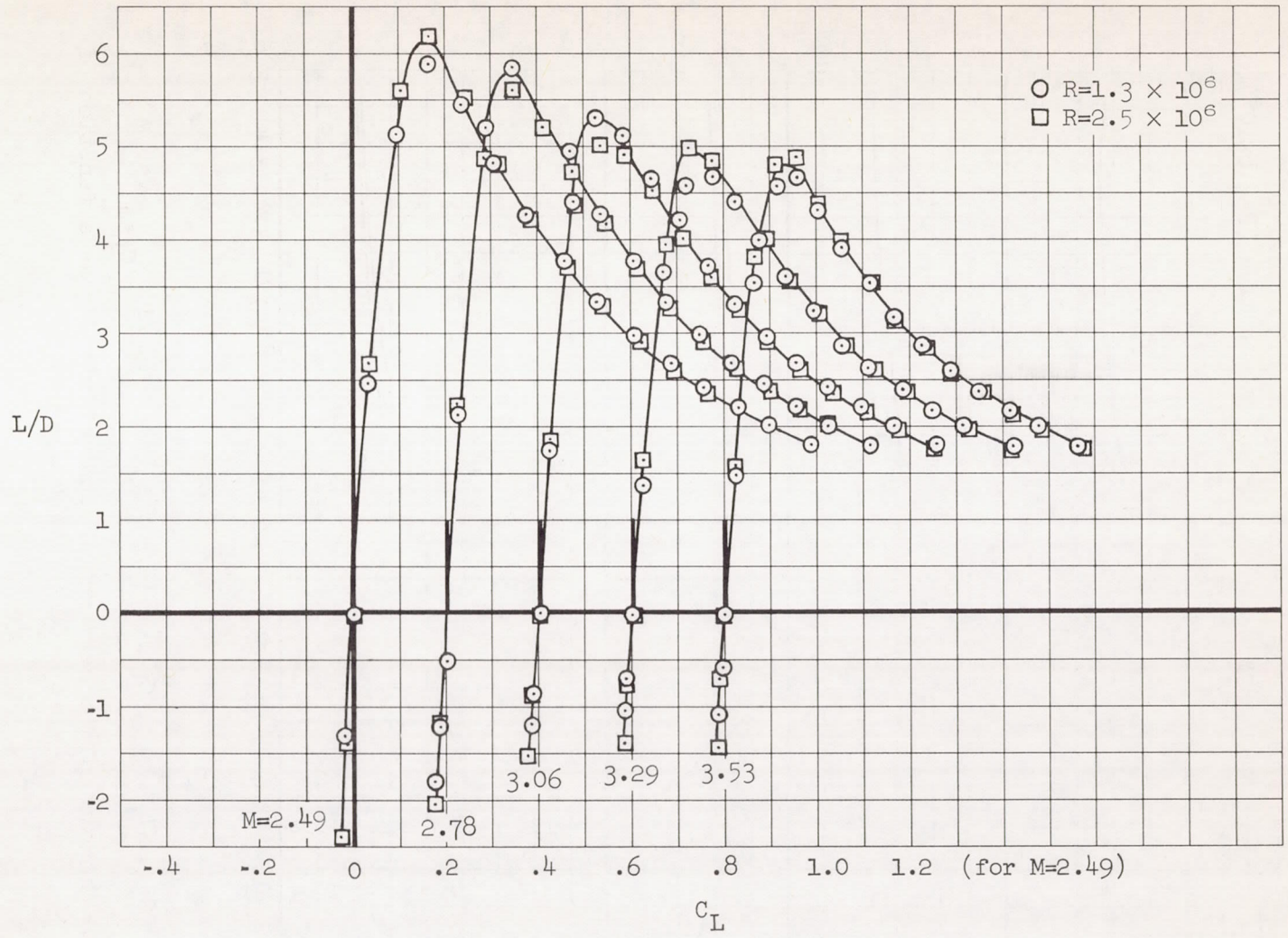

(d) $\frac{L}{D}$ vs. C_L

Figure 4.- Concluded.

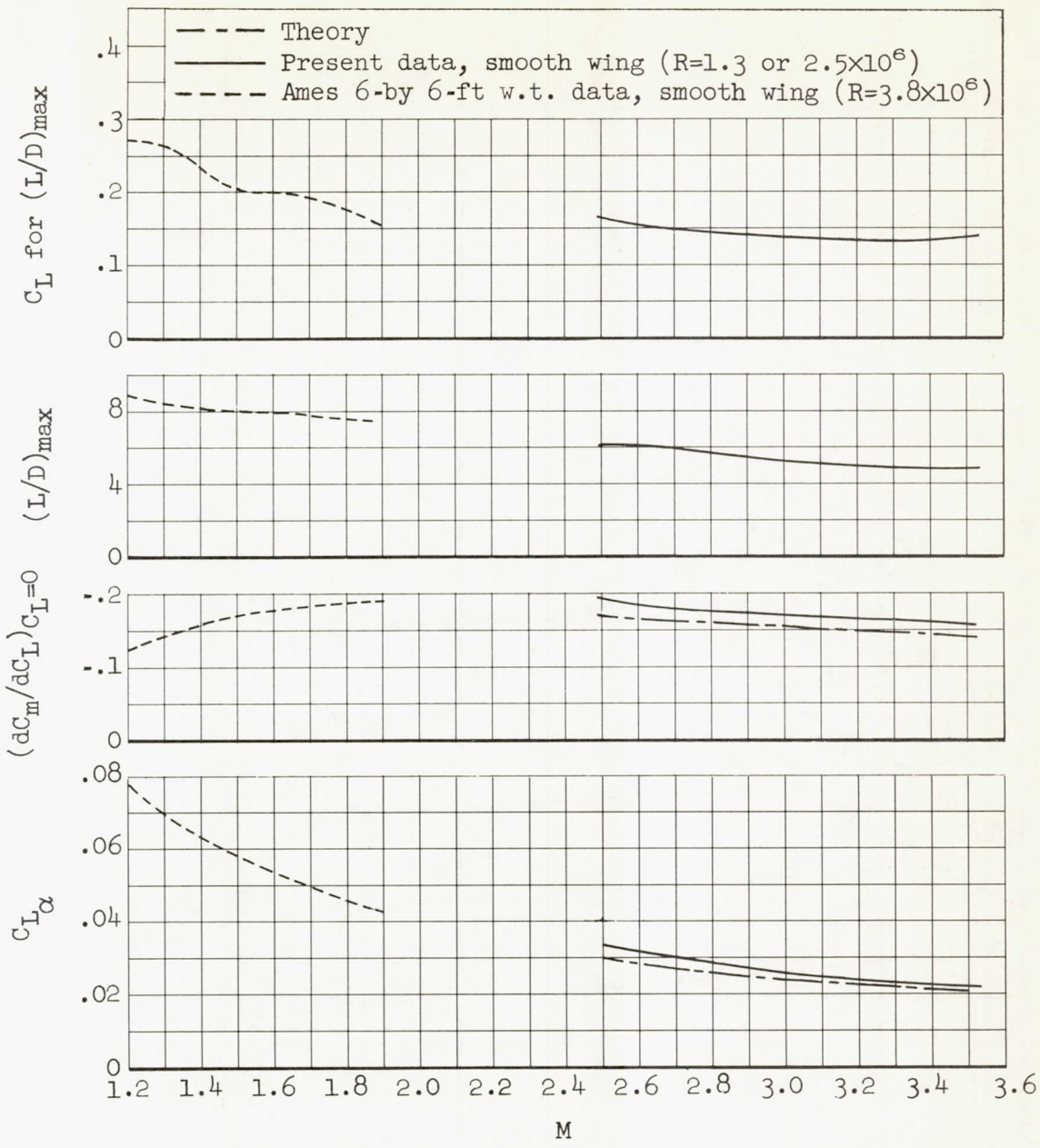

(a) C_{L_α}, $(L/D)_{max}$, C_L for $(L/D)_{max}$, and $(dC_m/dC_L)_{C_L=o}$ vs. M

Figure 5.- Summary of the aerodynamic characteristics as a function of Mach number.

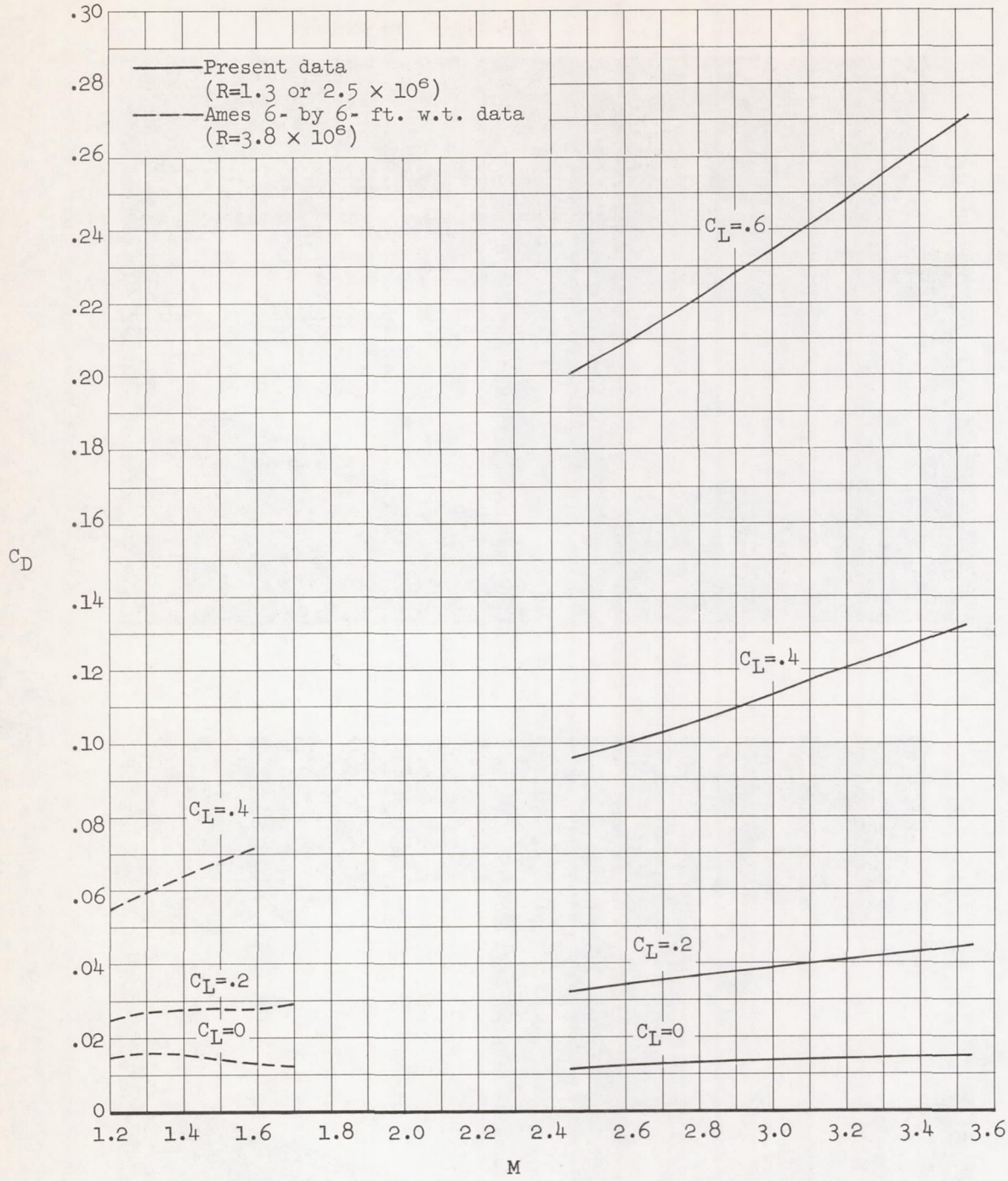

(b) C_D vs. M

Figure 5.- Concluded.

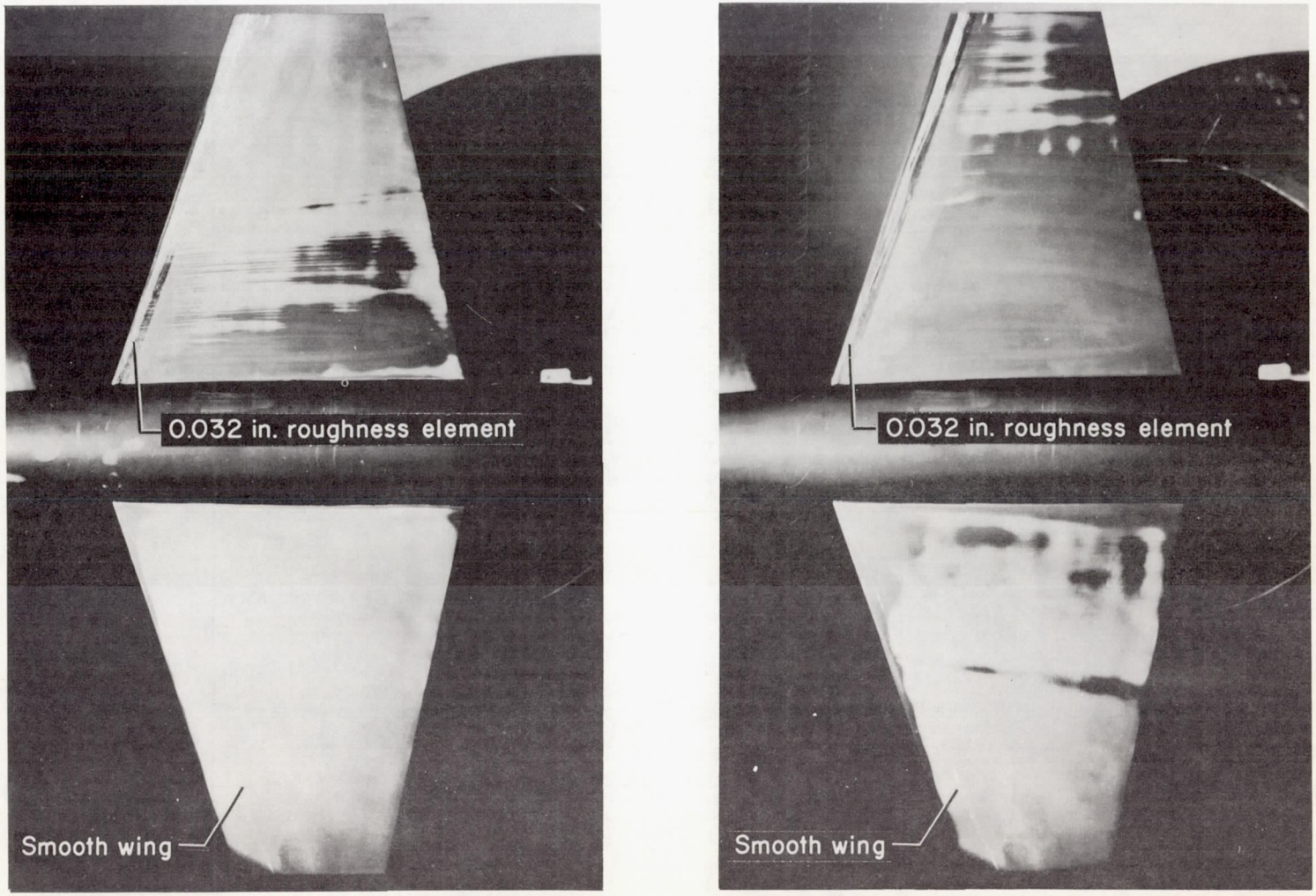

(a) R = 1.3×10^6; time = 20 min.

(b) R = 2.5×10^6; time = 44 min.

Figure 6.- Effect of different sizes of single-element roughness on the boundary-layer flow as indicated by azobenzene; M = 3.53, $\alpha = 0^\circ$.

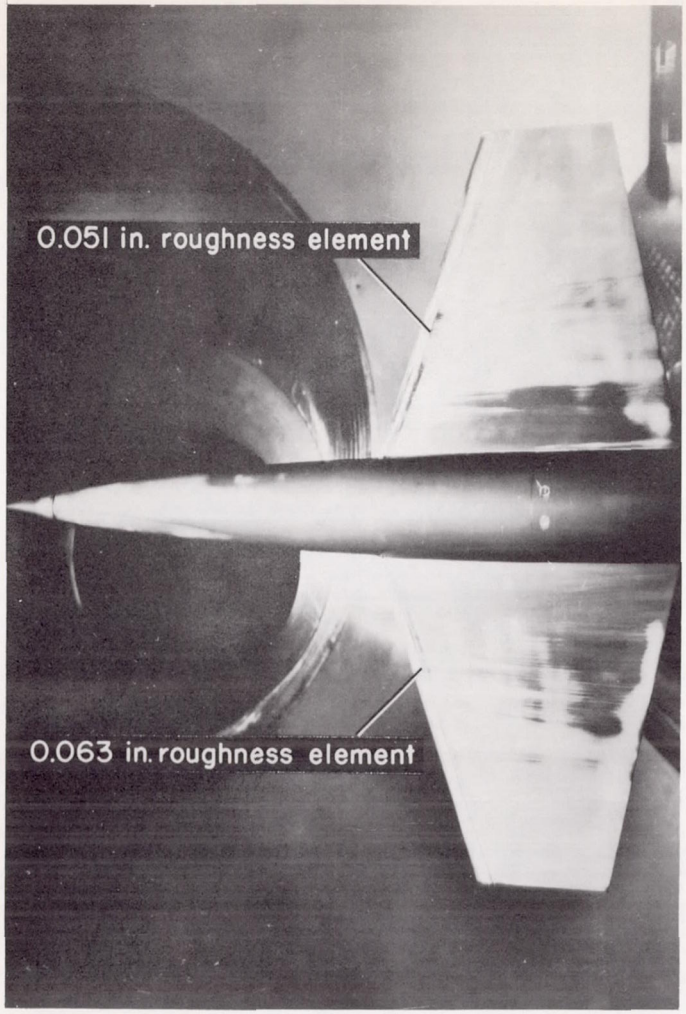

(c) R = 1.3×10^6; time = 20 min.

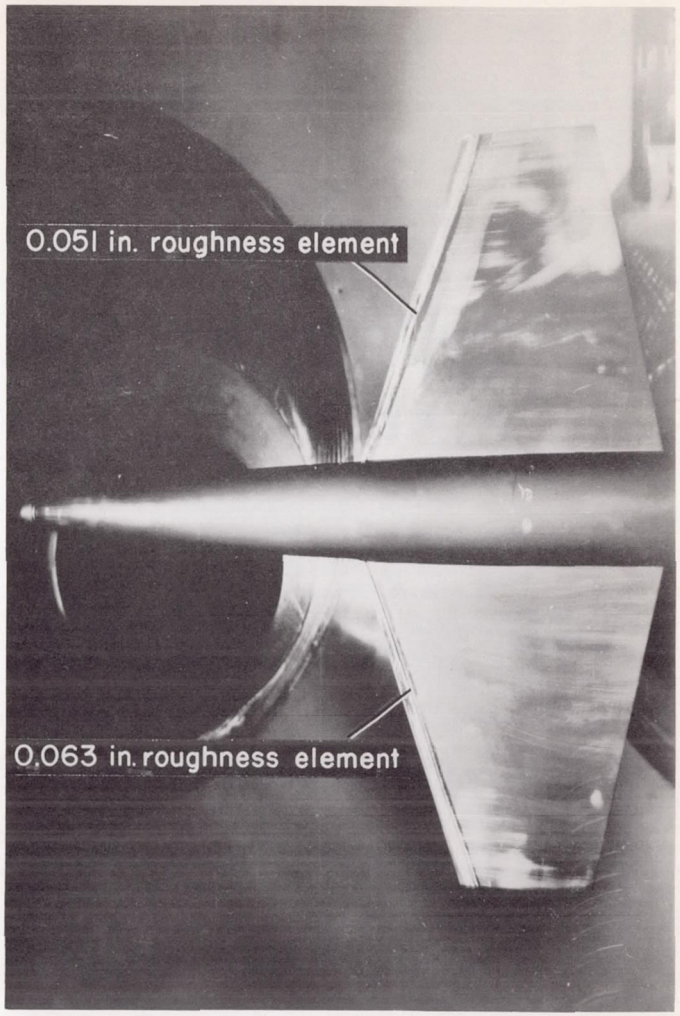

A-23917.1

(d) R = 2.5×10^6; time = 44 min.

Figure 6.- Concluded.